P. G. Hodge, Jr.
Department of Aerospace Engineering and Mechanics,
University of Minnesota,
Minneapolis, MN 55455

K.-J. Bathe
Department of Mechanical Engineering,
Massachusetts Institute of Technology,
Cambridge, MA 02139

E. N. Dvorkin
Universidad de Buenos Aires,
Facultad de Ingeniera,
Buenos Aires, Argentina

Causes and Consequences of Nonuniqueness in an Elastic/Perfectly-Plastic Truss

A complete solution to collapse is given for a three-bar symmetric truss made of an elastic/perfectly-plastic material, using linear statics and kinematics, and the solution is found to be partially nonunique in the range of contained plastic deformation. The introduction of a first-order deviation from symmetry and/or the inclusion of first-order nonlinear terms in the equilibrium equations is found to restore uniqueness. The significance of these effects is analyzed and discussed from mathematical, physical, modelling, computational, and engineering points of view.

1 Introduction

In the linear theory of elasticity the solution to a "well-defined boundary-value problem" is known to exist and be unique. However, for an elastic/perfectly-plastic material neither of these facts is obvious. Indeed, if the load is equal to the so-called "yield-point load" the solution ceases to be unique; beyond this load no solution exists.

The mathematical description of a boundary-value problem for an elastic/perfectly-plastic material involves partial differential equations and nonlinear constitutive relations. Further, if actual answers are required, it is necessary to approximate the structure with a numerical model. Thus the difficulty in combining mathematical rigor and physical intuition in the discussion of such questions as uniqueness is compounded by the necessity of distinguishing between the true nature of the continuum model and aspects introduced by the numerical model.

However, many features of the general continuum are present in much simpler structures where they can be more clearly discussed. As an illustration of this approach, the present paper is concerned with a particular simple three-bar plane truss.

We begin by defining a "well-defined equilibrium problem" for trusses as one in which the applied forces and displacements at the joints are such that:

(*a*) overall equilibrium is not violated;
(*b*) overall displacement constraints prescribe a unique allowable rigid-body motion (usually zero);
(*c*) at each joint in each of two independent directions either the displacement or the applied load is prescribed.

It is not difficult to prove that the solution to any well-defined equilibrium elasticity problem is unique. Indeed, if two solutions exist and are denoted by primes and double primes, then it follows from the principle of virtual work that

$$\Sigma_{\text{bars}}(F_i' - F_i'')(e_i' - e_i'') = \Sigma_{\text{joints}}(\mathbf{P}_j' - \mathbf{P}_j'')\cdot(\mathbf{u}_j' - \mathbf{u}_j'') \quad (1)$$

where F_i and e_i are the bar force and elongation, respectively, and $\mathbf{P}_j$ and $\mathbf{u}_j$ are the respective force and displacement vectors at joint j. If each solution satisfies condition (*c*) above and we write the scalar product in terms of components in the independent prescription directions, then either $P' = P''$ or $u' = u''$ in each term on the right. Further, if each bar is elastic, then

$$F_i = k_i e_i \quad (2)$$

where the stiffness k_i is positive. Thus equation (1) becomes

$$\Sigma_{\text{bars}} k_i (e_i' - e_i'')^2 = 0 \quad (3)$$

which clearly requires that each $e_i' = e_i''$ and hence each $F_i' = F_i''$. Equilibrium equations then show each $\mathbf{P}_j' = \mathbf{P}_j''$, and truss kinematics plus condition (*b*) above lead to each $\mathbf{u}_j' - \mathbf{u}_j'' = 0$. Therefore, the solution is unique.

Let us generalize the material behavior of equations (2) to an "elastic/perfectly-plastic" truss where each bar behaves elastically under small bar forces but can elongate indefinitely when F_i reaches a certain limiting value Y_i with similar behavior in compression. Thus during any sufficiently small time interval each bar is

EITHER
Elastic $\quad (F_i^2 < Y_i^2 \quad \text{AND } \Delta F_i = k_i \Delta e_i) \quad (4a)$
OR Plastic $\quad (F_i^2 = Y_i^2 \quad F_i \Delta e_i \geq 0) \quad (4b)$

Consider first any well-posed equilibrium boundary-value problem where any prescribed displacements are zero and the loads $\mathbf{P}_j$ are such that every bar is elastic. Clearly the same unique solution will hold as in the ideally elastic truss.

Now consider this same truss under the set of loads $\lambda \mathbf{P}_j$ where λ is slowly increased from $\lambda = 1$. So long as $F_i^2 < Y_i^2$ for each bar, the truss will remain fully elastic and the unique solution will increase in proportion to λ. However, for some critical value λ_e one or more bars will have their force

Contributed by the Applied Mechanics Division for presentation at the Winter Annual Meeting, Anaheim, CA, December 7–12, 1986, of the American Society of Mechanical Engineers.

Discussion on this paper should be addressed to the Editorial Department, ASME, United Engineering Center, 345 East 47th Street, New York, N.Y. 10017, and will be accepted until two months after final publication of the paper itself in the JOURNAL OF APPLIED MECHANICS. Manuscript received by ASME Applied Mechanics Division, November 27, 1984; final revision August 1, 1985. Paper No. 86-WA/APM-8.

$F_i = \pm Y_i$ and for larger values of λ some bars will be plastic. For a truss with a sufficient degree of indeterminancy enough bars remain elastic to support further increases in λ, but eventually a second critical value λ_L is reached at which the truss becomes a mechanism and no further load increases are possible.

Clearly the displacements of a mechanism motion are not unique, but the situation with regard to uniqueness is not as clear in the range of "contained plastic deformation" when $\lambda_e < \lambda < \lambda_L$. When even one bar reaches yield, the uniqueness proof above breaks down, since any two solutions which included plastic behavior for that bar would furnish $F_i' = F_i''$ but give no information about either e_i' or e_i''. In most examples and applications it turns out that uniqueness does hold in the range of contained plastic deformation, but extremely simple counter examples can be constructed in which more than one displacement solution exists for all loads with $\lambda > \lambda_e$.

In Section 2 we shall review a simple example of a 3-bar truss (Hode and White, 1980). In particular, we will note that any of several infinitesimal changes in the definition of the problem would render the solution unique up to $\lambda = \lambda_L$. In Sec. 3 we will examine one such variation by introducing an additional horizontal load αP, and we will study the limiting case as α tends to zero.

Section 4 will show that if we require equilibrium in the deformed position, rather than in the original configuration as is normally done in a linear analysis, then the change in predicted values can be expressed in terms of the small parameter $\beta = \sigma_y / E$ which is determined by the physical properties of the bar materials. The original problem now has a unique solution, but as α tends to zero in the varied problem, the predictions are quite different than in Section 3.

In Section 5 we attempt to solve the above models by the prepared computer program ADINA (1981). Finally, the paper concludes with a discussion of the relation between the various model solutions and the physical behavior to be expected from a "real" truss.

2 Nonunique 3-Bar Truss

The 3-bar truss in Fig. 1 has been used to point out many interesting facets of elastic/plastic truss behavior (Hodge and White, 1980; Hodge, 1958; Prager, 1948; Freudenthal, 1954). All bars have the same Young's modulus E and cross-sectional area A, but the yield stress for the diagonal bars is σ_y whereas that for the vertical bar is 3 σ_y. We begin by using an asterisk to define all real physical variables and defining dimensionless quantities as follows:

$$\beta = \sigma_y / E \qquad P = P^*/A\sigma_y \qquad F_i = F_i^*/A\sigma_y$$
$$u = u^*/\beta H \qquad v = v^*/\beta H \qquad e_i = e_i^*/\beta H \tag{5}$$

where H is defined in Fig. 1.

The static and kinematic equations are trivial and can be written in incremental form as

$$\Delta F_1 - \Delta F_3 = 0 \tag{6a}$$
$$\Delta F_1 + \Delta F_3 + \sqrt{2}\Delta F_2 = \sqrt{2}\Delta P \tag{6b}$$
$$\Delta e_1 = (\Delta v + \Delta u)/\sqrt{2} \quad \Delta e_2 = \Delta v \quad \Delta e_3 = (\Delta v - \Delta u)/\sqrt{2} \tag{7}$$

Equations (4) and (7) can be combined for each bar to obtain

Bar 1	Elastic	$-1 < F_1 < 1$	$\Delta F_1 = (\Delta v + \Delta u)/2$		(8a)
	Plastic	$F_1 = \pm 1$	$\Delta F_1 = 0$	$F_1(\Delta v + \Delta u) > 0$	(8b)
Bar 2	Elastic	$-3 < F_2 < 3$	$\Delta F_2 = \Delta v$		(8c)
	Plastic	$F_2 = \pm 3$	$\Delta F_2 = 0$	$F_2 \Delta v > 0$	(8d)
Bar 3	Elastic	$-1 < F_3 < 1$	$\Delta F_3 = (\Delta v - \Delta u)/2$		(8e)
	Plastic	$F_3 = \pm 1$	$\Delta F_3 = 0$	$F_3(\Delta v - \Delta u) > 0$	(8f)

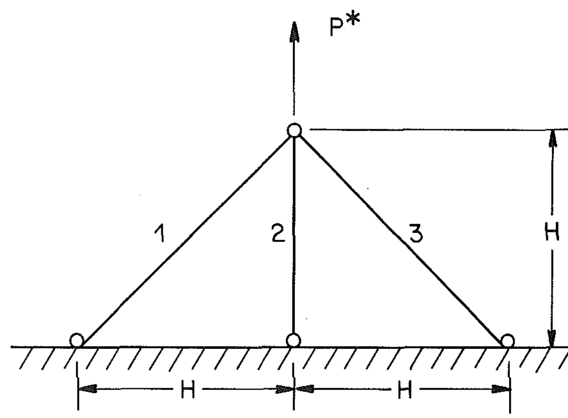

Fig. 1 Three-bar truss with vertical load

As the load P is slowly increased from zero, all three bars will start from zero force and be elastic, hence we can use the integrated form of equations (6) and (8a,c,e) to obtain

Stage 1

$$u = 0 \quad v = F_2 = (2 - \sqrt{2})P \quad F_1 = F_3 = (1 - 1/\sqrt{2})P \tag{9}$$

In view of the different yield stresses, the diagonal bars will yield first, and the limit of Stage 1 is

Stage 1L

$$P = 2 + \sqrt{2} \quad u = 0 \quad v = F_2 = 2 \quad F_1 = F_3 = 1 \tag{10}$$

As the load P is further increased both diagonal bars will yield, hence we use equations (8b, c, f) with equations (6). However, these equations are not independent since equations (8b, f) show that $\Delta F_1 = \Delta F_3 = 0$ which automatically satisfies equation (6a). The five equations (8b, c, f) and (6 a, b) do provide unique values for the increments of forces and vertical displacement, but only provide bounds for the horizontal displacement:

Stage 2

$$\Delta F_1 = \Delta F_3 = 0 \quad \Delta F_2 = \Delta v = \Delta P \quad -\Delta P \leq \Delta u \leq \Delta P \tag{11}$$

Adding these increments to equations (10) and determining P so that $F_2 = 3$, we obtain the limiting solution

Stage 2L

$$P = 3 + \sqrt{2} \quad F_1 = F_3 = 1 \quad F_2 = v = 3 \quad -1 \leq u \leq 1 \tag{12}$$

At this load all bars are plastic. Equations (8b, d, f) now automatically satisfy both of (6) with $\Delta P = 0$, hence the mechanism motion at the yield-point load has two degrees of freedom with Δu and Δv subject only to inequalities

Stage 3 (mechanism)

$$P = 3 + \sqrt{2} \quad F_1 = F_3 = 1 \quad F_2 = 3$$
$$\Delta v \geq 0 \quad -\Delta v \leq \Delta u \leq \Delta v \tag{13}$$

The nonuniqueness of the motion in Stage 3 has been long known and is implied in the very name of mechanism. However, the nonuniqueness in Stage 2, when the truss is still capable of handling increased load is a more subtle phenomenon. It can be examined from mathematical, physical, computational, or modelling points of view.

Mathematically, it occurs because the simultaneous occurance of yield in two bars at stage 1L leads to the homogeneous equilibrium relation (equation (6a)) becoming redundant in Stage 2. Thus the total system of 5 equations becomes singular and cannot be solved uniquely.

Physically, we could think of the general motion permitted in Stage 2 as a combination of a vertical motion $\Delta v = \Delta P$ which stretches each plastic bar by an amount $\Delta v/\sqrt{2}$, together with a horizontal motion Δu. If Δu were positive, this latter

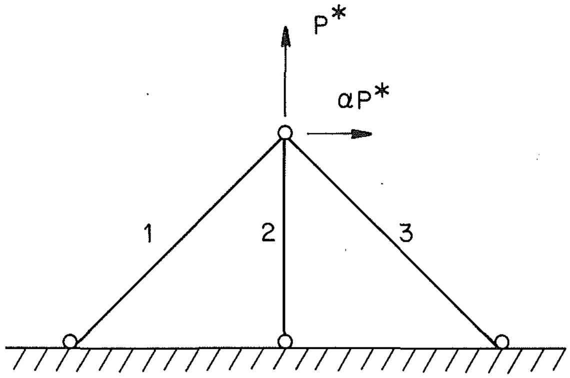

Fig. 2 Truss with small horizontal load component

motion by itself would compress bar 3 which would not be permissible at tensile yield. However, the physical requirement of extension applies only to the total motion which includes a positive Δv, hence the only restriction is given by the inequalities in equation (11). The computational aspects will be discussed in Section 5.

From a modelling viewpoint, any of several infinitesimal changes in the model will remove the singularity, produce a unique value for u, and create at most infinitesimal changes in the other variables. If the symmetry of the problem is changed ever-so-slightly by an alteration of area, stiffness, strength, load, or node position, then bar 1, say, will become plastic while bar 3 is still just short of yield. Then Stage 3 would use equations (8*b*, *c*, *e*); equation (6*a*) would no longer be an identity, but would contribute the information $\Delta F_3 = 0$; equation (8*e*) would then provide the unique solution

$$\Delta u = \Delta v \qquad (14)$$

Further, since $\Delta F_3 = 0$, Stage 2 would continue as before until bar 2 yielded. The resulting mechanism motion would have one degree of freedom with bar 3 rotating as a rigid body subject to equation (14) corresponding to the right-hand limit of the last inequality in equation (13).

However, if the change from symmetry is in the opposite sense, bar 3 will yield while bar 1 remains elastic and equation (14) will be replaced by

$$\Delta u = -\Delta v \qquad (15)$$

corresponding to the left-hanf inequality in equation (13).

Another possibility is to allow for infinitesimal strain hardening. If both bars 1 and 3 harden equally, the symmetric solution $\Delta u = 0$ will become unique, but if there is any difference in the hardening of bars the solution will still be unique but any value of u satisfying equation (11) may be obtained by a suitable ratio of the hardening coefficients.

Uniqueness of solution will also result if we account for the additional stiffening effect of the bars produced by their elastic elongation. However, we will postpone discussion of this effect until we have examined in detail the consequences of altering symmetry in a specific manner in the next section.

3 Truss with Small Horizontal Load Added

Let us suppose that as before the truss geometry in Fig. 1 is precisely symmetric, that bars 1 and 3 are identical in all their measurements and properties, and that there is absolutely no strain hardening. However, let us allow for a minute deviation in the direction of the applied load. Thus instead of the problem in Fig. 1, we consider the truss problem in Fig. 2, where α is a small, dimensionless parameter; for definiteness we take $\alpha > 0$.

Equations (6*b*) and (8) are still applicable, but equation (6*a*) is replaced by

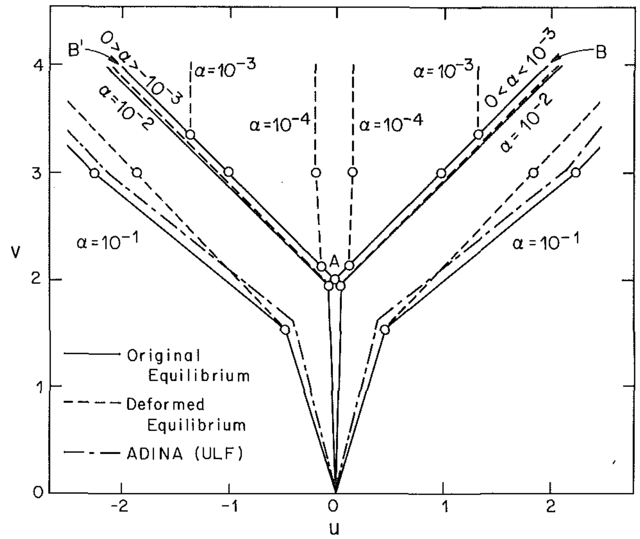

Fig. 3 Motion of loaded point

$$\Delta F_1 - \Delta F_3 = \sqrt{2}\alpha \Delta P \qquad (16)$$

The fully elastic solution is obtained from equation (6*b*), (16), and (8*a,c,e*):

Stage 1

$$u = \sqrt{2}\alpha P \qquad v = F_2 = (2 - \sqrt{2})P$$
$$F_1 = (1 - 1/\sqrt{2} + \alpha/\sqrt{2})P \qquad F_3 = (1 - 1/\sqrt{2} - \alpha/\sqrt{2})P \qquad (17)$$

For any positive α, bar 1 yields first with the following values:

Stage 1*L*

$$P = (2 + \sqrt{2})[1 - (\sqrt{2} + 1)\alpha]$$
$$u = 2(\sqrt{2} + 1)\alpha \qquad v = F_2 = 2 - 2(\sqrt{2} + 1)\alpha \qquad (18)$$
$$F_1 = 1 \qquad F_3 = 1 - 2(\sqrt{2} + 1)\alpha$$

where we have kept only first-order terms in α.

With bar 1 plastic we use the equations (8*b*, *c*, *e*), (6*b*), and (16) to obtain the incremental solution:

Stage 2

$$\Delta u = [1 + (1 + 2\sqrt{2})\alpha]\Delta P \qquad \Delta v = \Delta F_2 = (1 + \alpha)\Delta P$$
$$\Delta F_1 = 0 \qquad \Delta F_3 = -\sqrt{2}\alpha \Delta P \qquad (19)$$

We note that ΔF_3 is negative, and hence for α reasonably small bar 3 will remain elastic. Therefore, Stage 2 ends when bar 2 becomes plastic:

Stage 2*L*

$$\Delta P = 1 + (2\sqrt{2} + 1) \qquad P = 3 + \sqrt{2} - (3 + \sqrt{2})\alpha$$
$$u = 1 + 2(3\sqrt{2} + 2)\alpha \qquad v = F_2 = 3 \qquad (20)$$
$$F_1 = 1 \qquad F_3 = 1 - (3\sqrt{2} + 2)\alpha$$

In Stage 3 bars 1 and 2 are plastic. Equations (6*b*), (8*b*, *d*, *e*), and (16) cannot be solved for a prescribed P but require the following:

Stage 3 (mechanism)

$$\Delta P = \Delta F_1 = \Delta F_2 = \Delta F_3 = 0 \qquad \Delta v = \Delta u \geq 0 \qquad (21)$$

Clearly this is a mechanism motion under the yield-point load $P_L = (3 + \sqrt{2})(1 - \alpha)$.

The solid curves in the right half of Fig. 3 show the motion of the loaded point for various α. To the scale used values of $\alpha < 10^{-3}$ will not be any different than $\alpha = 10^{-3}$. In particular, the curve OAB will also be the limit curve as α tends to zero from above.

The preceding analysis is for the case $\alpha > 0$. Clearly, if $\alpha < 0$, i.e., if the horizontal component is directed to the left, the

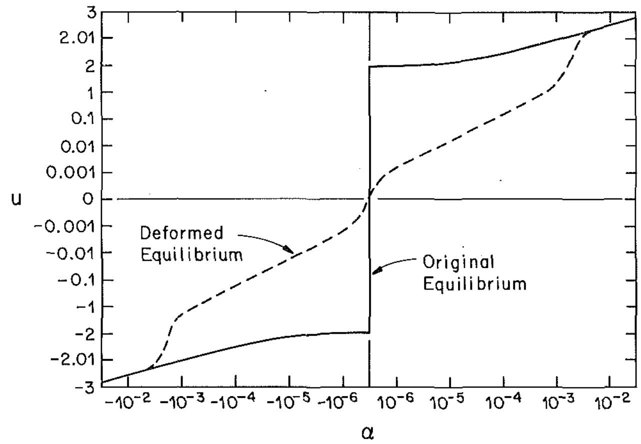

Fig. 4 Horizontal displacement as a function of α for $v=4$

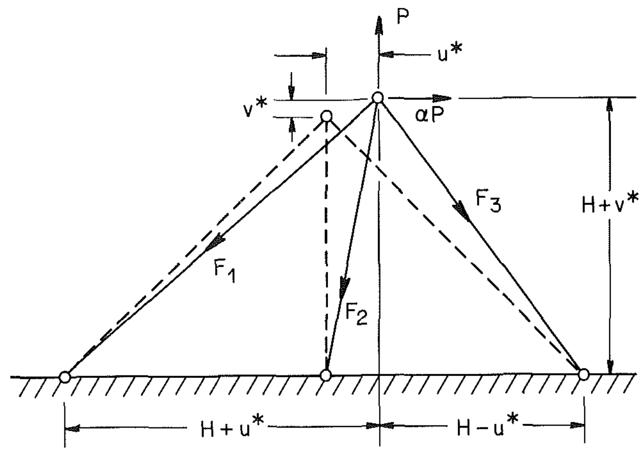

Fig. 5 Equilibrium of deformed truss

roles of bars 1 and 3 will be interchanged and the sign of u will be reversed. In particular, we obtain curve OAB′ as the limit curve when α tends to zero from below.

Both OAB and OAB′ are admissible curves for the nonunique solutions obtained in Section 2 where α is set equal to zero at the outset. Indeed, any curve in the open wedge B′AB whose slope satisfies $dv \geq |du|$ is an admissible nonunique solution to that ideal problem.

The solid curve in Fig. 4 shows the horizontal displacement u as a function of α when the vertical displacement is $v=4$. Note that both scales are nonlinear. It is clear from either Fig. 3 or Fig. 4 that the motion is unique for any fixed positive value of α, hence the horizontal displacement u is a unique function of the load P. Furthermore, as the parameter α tends to zero, this motion will approach a unique limit which is very close to its value when $\alpha=10^{-3}$. The same statements apply to negative values of α, but the two limits are distinctly different. Finally, a direct analysis with $\alpha=0$ leads to a nonunique solution which includes all possibilities between the two above limits. These points will be commented on further in Section 6.

4 Deformed Equilibrium Approach

The geometrically linear theory used in the two preceding sections is based on the neglect of various small quantities. However, as we have seen, small values of the horizontal load parameter α can have a large effect on the motion of the truss vertex. Therefore, it seems natural to ask if any of the neglected small effects might have large consequences. In particular, we consider the change in effective stiffness due to small displacements. Since Fig. 1 can be treated as the special case $\alpha=0$, we examine this effect for the truss in Fig. 2 by replacing the equilibrium relations (equations (16) and (6*b*)) with equilibrium requirements derived from Fig. 5. Using the same dimensionless variables and keeping only first order terms in the small parameter β, we obtain

$$\begin{aligned} \Delta F_1 - \Delta F_3 + (\beta/2)[(F_3+F_1+2\sqrt{2}F_2)\Delta u \\ + (F_3-F_1)\Delta v] = \sqrt{2}\alpha\Delta P \\ \Delta F_1 + \Delta F_3 + \sqrt{2}\Delta F_2(\beta/2)[(F_3-F_1)\Delta u \\ + (F_3+F_1)\Delta v] = \sqrt{2}\Delta P \end{aligned} \quad (22)$$

For simplicity, we continue to use the linear equations (8); the introduction of nonlinear terms there would not change the qualitative results.

Strictly speaking, equations (22) are nonlinear differential equations. Since the nonlinear terms are all multiplied by the small parameter β, we shall linearize them by using appropriate constant values for the forces in the terms multiplied by β. In effect, we replace the differential equation by taking a single linear difference equation for each stage of the solution.

We regard both α and β as small compared to unity and neglect all terms α^2, $\alpha\beta$, β^2, etc. Therefore, we need only the zero-order terms for the forces in equations (22). At the end of Stage 1, it follows from equations (18) that the zero-order forces are $F_1=F_3=1$, $F_2=2$. since all $F_i=0$ at the beginning of the stage, their average values during Stage 1 are

$$F_1=F_3=\tfrac{1}{2} \quad F_2=1 \quad (23)$$

The solution of equations (22) and (8*a*, *c*, *e*) with F_i given by equation (23) is

Stage 1

$$\begin{aligned} &\Delta u=\sqrt{2}\alpha\Delta P \quad \Delta v=\Delta F_2=\sqrt{2}(\sqrt{2}-1)[1-(\sqrt{2}-1)\beta/2]\Delta P \\ &\Delta F_1=[(\sqrt{2}-1)/\sqrt{2}][1-(\sqrt{2}-1)\beta/2+(\sqrt{2}+1)\alpha]\Delta P \\ &\Delta F_3=[(\sqrt{2}-1)/\sqrt{2}][1-(\sqrt{2}-1)\beta/2-(\sqrt{2}+1)\alpha]\Delta P \end{aligned} \quad (24)$$

The stage ends when bar 1 becomes plastic at the load

Stage 1*L*

$$P=(2+\sqrt{2})[1+(\sqrt{2}-1)\beta/2-(\sqrt{2}+1)\alpha] \quad (25)$$

With this load, the forces and displacements at Stage 1*L* all have the same values as in equations (18) for the geometrically linear theory (to within first-order terms).

In Stage 2, bar 1 is plastic and, to zero-order terms, $F_1=F_3=1$ throughout the stage. Therefore, using (8*b*, *c*, *e*) we can write equation (22) as

$$\begin{aligned} &[1+2\beta(1+\sqrt{2}F_2)]\Delta u - \Delta v = 2\sqrt{2}\alpha\Delta P \\ &-\Delta u + [(1+2\sqrt{2})+2\beta]\Delta v = 2\sqrt{2}\Delta P \end{aligned} \quad (26)$$

where we have not yet assigned a value to F_2, but have treated it as a constant. To within first-order terms the solution of equation (26) is

Stage 2

$$\Delta u = \{1+(1+2\sqrt{2})\alpha - [(2+\sqrt{2})+(1+2\sqrt{2})F_2]\beta\}\Delta P \quad (27a)$$

$$\Delta v = \Delta F_2 = [1+\alpha-(\sqrt{2}+F_2)\beta]\Delta P \quad (27b)$$

$$\Delta F_1 = 0 \qquad \Delta F_3 = [(1+\sqrt{2}F_2)\beta - \sqrt{2}\alpha]\Delta P \quad (27c,d)$$

The essential difference between equations (27) and equations (19) for the linear case is that now F_3 will increase for *sufficiently small* α *so that it is not clear whether bar 2 or bar 3* will be the next to yield. Therefore, we consider the two cases separately. If bar 2 yields next, the final value of F_2 is $F_2=3$ hence its average value during the stage is $F_2=2.5$. The solution at the end of the stage is then

Stage 2*LA*

$$\Delta P = 1+(2\sqrt{2}+1)\alpha+(\sqrt{2}+5/2)\beta \quad (28a)$$

$$\Delta F_3 = (1+5\sqrt{2}/2)\beta - \sqrt{2}\alpha \quad (28)b)$$

$$F_1=1 \quad F_2=3 \quad P=3+\sqrt{2} \quad u=1 \quad v=3 \quad (28c)$$

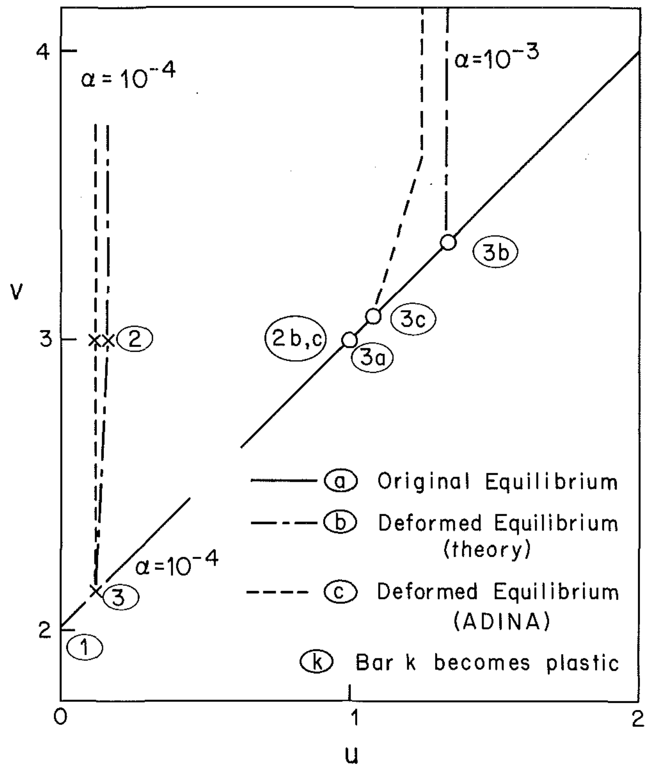

Fig. 6 Comparison of computational and theoretical results

$$F_3 = 1 + (1+5/\sqrt{2})\beta - (3\sqrt{2}+2)\alpha \le 1 \tag{28d}$$

$$t \equiv \alpha/\beta \ge (13-2\sqrt{2})/14 = 0.727 \tag{28e}$$

In equations (28) we have listed only the zero order terms for P, u, and v, but the first order terms are important for F_3, since this solution is valid only if $F_3 \le 1$, thus leading to inequality (28) on the ratio $t=\alpha/\beta$ which may be of any magnitude.

In Stage 3*A*, bars 1 and 2 are at yield and equations (22) and (8*b*, *d*, *e*) lead to

$$\Delta F_3 = (\Delta v - \Delta u)/2 \tag{29a}$$

$$\Delta u - \Delta v + \beta[(F_3+1+6\sqrt{2})\Delta u + (F_3-1)\Delta v] = 2\sqrt{2}\alpha\Delta P \tag{29b}$$

$$\Delta v - \Delta u + \beta[(F_3-1)\Delta u + (F_3+1)\Delta v] = 2\sqrt{2}\Delta P \tag{29c}$$

For bar 3 to reach yield will require only a first order increase in F_3, hence to order zero $\Delta u = \Delta v$ and equation (29*c*) shows that ΔP is of order greater than zero. Therefore, keeping only the leading terms in each equation (29) we see that for bar 3 to reach yield

$$\Delta F_3 = (\Delta v - \Delta u)/2 = (3\sqrt{2}+2)\alpha - (5/\sqrt{2}+1)\beta \tag{30a}$$

Since this is first order, equation (29*c*) shows that ΔP is also of first order. Keeping only the leading terms in equations (29), we obtain

$$\Delta u - \Delta v + \beta[(2+6\sqrt{2})\Delta u] = 0 \tag{30b}$$

$$\Delta u - \Delta v + \beta(2)\Delta v = 2\sqrt{2}\Delta P \tag{30c}$$

which leads to

Stage 3*LA*

$$\Delta u = \Delta v = (1/34)[(32+6\sqrt{2})t - (28+\sqrt{2})]$$
$$u = (1/34)[(32+6\sqrt{2})t + (6-\sqrt{2})]$$
$$v = (1/34)[(32+6\sqrt{2})t + (74-\sqrt{2})]$$
$$F_1 = 1 \quad F_2 = 3 \quad F_3 = 1 \quad P = 3+\sqrt{2} \tag{31}$$

to zero order terms.

The final stage occurs when all bars are plastic. Equations (8*b*, *d*, *f*) and (22) now lead simply to

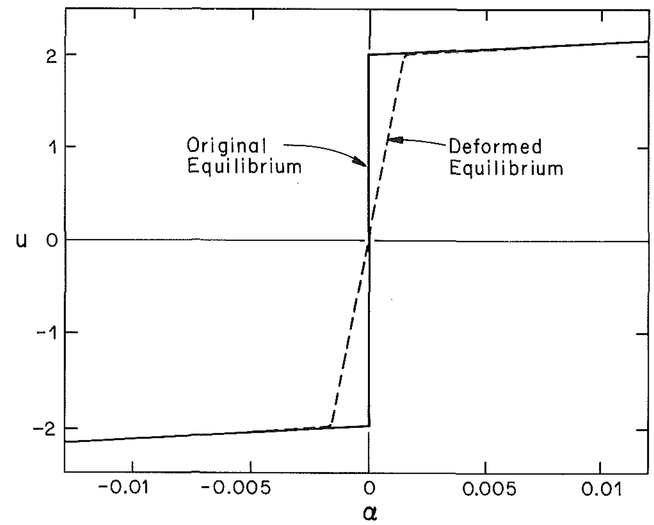

Fig. 7 Horizontal displacement as a function of α for v = 4

Stage 4

$$\Delta u = (t/17)(6-\sqrt{2})\Delta P$$
$$\Delta v = \sqrt{2}\Delta P/\beta \tag{32}$$

Thus, although we do not have a mechanism in the sense of linear plasticity, only a first order increase in ΔP is required to produce a zero-order vertical displacement.

Returning now to the case where bar 3 yields before bar 2, we do not know the final value of F_2, but we can denote it (to zero-order terms) by $2+\Delta F_2$. Therefore, the average value called for in equations (27) will be

$$F_2 = 2 + \Delta F_2/2 = 2 + \Delta P/2 \tag{33}$$

where the last step follows from equation (27*b*). It then follows from equation (27*d*) that when bar 3 yields

$$\Delta F_3 = \{[1+\sqrt{2}(2+\Delta P/2)]\beta - \sqrt{2}\alpha\}\Delta P = 2(\sqrt{2}+1)\alpha \tag{34}$$

This is a quadratic equation for ΔP whose solution is

Stage 2*LB*

$$\Delta P = [4.5+2\sqrt{2}+\sqrt{2}t+t^2]^{1/2} - (2+1/\sqrt{2}-t) \tag{35a}$$

$$\Delta u = \Delta v = \Delta F_2 = \Delta P \quad F_2 = 2+\Delta P \tag{35b}$$

where we have listed only the zero-order terms. In order for this solution to be valid, ΔF_2 cannot exceed 1, and it is readily verified that this requirement leads to the reverse of inequality (28):

$$t \le (13-2\sqrt{2})/14 \tag{35c}$$

In Stage 3*B*, bars 1 and 3 yield, and equations (22) and (8*b*, *c*, *f*) produce

$$\Delta F_2 = \Delta v$$
$$\beta(1+\sqrt{2}F_2)\Delta u = \sqrt{2}\alpha\Delta P \tag{36}$$
$$(\sqrt{2}+\beta)\Delta v = \sqrt{2}\Delta P$$

In view of equations (35*a*), the value of F_2 to be used in equation (36) is

$$F_2 = (1/2)[3 - 1/\sqrt{2} + t + (4.5+2\sqrt{2}+\sqrt{2}t+t^2)^{1/2}] \tag{37}$$

The solution (equation (36) when ΔF_2 is sufficient to bring F_2 to its yield value of 3) is

Stage 3*LB*

$$\Delta v = \Delta F_2 = \Delta P = 3 + 1/\sqrt{2} - t - (4.5+2\sqrt{2}+\sqrt{2}t+t^2)^{1/2}$$
$$\Delta u = 2t\Delta P/[3+1\sqrt{2}+t+(4.5+2\sqrt{2}+\sqrt{2}t+t^2)^{1/2}]$$

Since all three bars are now at yield, the incremental solution for Stage 4 is again given by equations (32).

The dashed curves in Figs. 3 and 4 show the displacements according to the nonlinear geometry model with $\beta = 10^{-3}$. As α tends to zero the displacements do move continuously with u being positive for $\alpha > 0$, zero for $\alpha = 0$, and negative for $\alpha < 0$. We shall comment more fully on the similarities and differences between the two solutions in the conclusions.

5 ADINA Solutions

The truss in Figs. 1 and 2 was run on the structural program ADINA (1981) for $\alpha = 0$ (no horizontal load as in Fig. 1) and for $\alpha = 10^{-6}$, 10^{-5}, 10^{-4}, 10^{-3}, 10^{-2}, and 10^{-1}. Default options were used for most of the parameters in ADINA, except as noted in the following discussion. All problems were run twice; once with a "material-nonlinear-only" (MNO) code corresponding to the analysis in Sections 2 and 3, and once with an "updated-Lagrangian-formulation" (ULF) code similar to the analysis in Section 4. Descriptions of these methods may be found in Bathe (1982).

For the case $\alpha = 0$ the MNO program only gave results up to the load $P = 3.415$, at which point it stopped with the message "NONPOSITIVE PIVOT FOR EQUATION 1 . . .COLLAPSE LOAD OF THE MODEL HAS BEEN REACHED." A load increment $P = 0.001$ was used, and the final values were

$$P = 3.415 \quad u = 0 \quad v = 2.00078$$
$$F_1 = F_3 = 1.00000 \quad F_2 = 2.0078 \tag{38}$$

with bars 1 and 3 being listed as PLASTIC. Clearly these values are an excellent approximation to those given in equation (10) for Stage $1L$, but they do not represent the collapse load given in equation (12).

The reason that the computer solution stops here is easy to see. ADINA, like most finite-element programs, essentially substitutes the appropriate equations (8) in equations (6) and then solves the resulting set of linear equations for Δu and Δv. However, for the next load increment we must use equations (8b, d, e) for which equations (6) become

$$0 \cdot \Delta u + 0 \cdot \Delta v = 0$$
$$0 \cdot \Delta u + \sqrt{2} \cdot v = \sqrt{2} P \tag{39}$$

Although these equations do contain the useful information $\Delta v = \Delta P$ given in equation (11), the stiffness matrix (the matrix of coefficients on the left-hand side of equation (39)) is singular. Therefore, standard methods of automatic solution will not produce the solution in equation (12). Such a singular matrix always occurs at the yield-point (collapse) load and its occurance due to nonuniqueness was evidently not allowed for when ADINA was written.

For $\alpha = 10^{-6}$, the MNO program stops with the same message and values, except that $u = 0.241477 \times 10^{-4}$. Evidently the small horizontal load gets "lost" in the computations leading to the stiffness matrix.

Two variations were experimented with to overcome this difficulty. When load steps near 3.414 were reduced to 0.0001, bar 1 became plastic at $P = 3.4143$. Although it took 19 iterations for this solution to converge, the program then continued with only one iteration per step until the load was $P = 4.415$ when it stopped with the message "ITERATION LIMIT REACHED WITH NO CONVERGENCE."

The other variation used an optional iteration method known as Broyden-Fletcher-Goldfarb-Shanno (BFGS) instead of the modified Newton method which is the default option (Bathe, 1982, Sec. 8.6). With BFGS, we obtained the same loads, but it took only 3 iterations to pass $P = 3.4143$, and when the program stopped at the collapse load the message was again "NONPOSITIVE PIVOT . . . . ".

For $\alpha = 10^{-5}$, the MNO program predicted that only bar 1 became plastic at $P = 3.415$ and continued to the load 4.414 with the values

$$P = 4.414 \qquad u = 0.999955 \qquad v = 2.99983$$
$$F_1 = 1.00000 \qquad F_2 = 2.99983 \qquad F_3 = 0.999938 \tag{40}$$

in excellent approximation to equations (20). The program then stopped with the message "ITERATION LIMIT REACHED WITH NO CONVERGENCE." The iteration limit was 9999 and the previous maximum number of iterations required was 17 when bar 1 became plastic.

Similar results were obtained for all $\alpha \geq 10^{-4}$. In all cases the numbers produced by ADINA using the MNO model were in excellent agreement with the formulas in Sections 2 and 3.

Using ULF with $\alpha = 0$ we did not encounter any singularities and the program ran all the way to $P = 4.5$, the largest load requested. The displacement u was always identically zero, and bars 1 and 3 both became plastic at $P = 3.415$. The solution at $P = 3.415$ took only 3 iterations, but at $P = 4.415$ it took over 4000 iterations before the solution was found for all three bars plastic, and from then on it took about 20 iterations per step. All numbers were in close agreement with the results of Section 4 with $\alpha = 0$. When we ran the same program with BFGS iteration, the same numbers were obtained but the maximum number of iterations was three.

Figure 6 compares the motion of the loaded vertex according to the ADINA results and the theory in Sections 2 through 4 for $\alpha = 10^{-3}$ and $\alpha = 10^{-4}$. According to the MNO model bar 3 never does become plastic and the mechanism motion is simply $\Delta u = \Delta v$ once $P = 4.414$. ADINA gives the same results up to collapse of $P = 4.414$ but does not, of course, predict the mechanism motion.

For the ULF model when $\alpha = 10^{-3}$ equations (29) for Stage 3 apply only during a load increment $\Delta P = 0.0015$. Since the load step used in ADINA was only 0.001, it is perhaps not surprising that the predicted horizontal displacements are noticeably different, as shown in Fig. 6. It is not clear whether this is due to the numerical approximations in ADINA or to the approximate integration assumed in interpreting the difference equations in Section 4.

A lesser difference is observed for $\alpha = 10^{-4}$, as shown in Fig. 6. For $\alpha = 10^{-5}$ and $\alpha = 10^{-6}$, the predicted values of u are too small to appear on the scale of Fig. 6.

For $\alpha = 10^{-2}$ the results predicted by ADINA lie very close to the corresponding curve in Fig. 3.

Finally, for $\alpha = 10^{-1}$, ADINA's results are noticeably different from those predicted in Section 4, as indicated by the dot-dash curve in Fig. 3. Since the latter equations were all linearized with respect to α, it is to be expected that they may be significantly in error for α as large as 0.1. For example, a neglected term in α^2 might be considerably larger than a considered term in β.

6 Conclusions

The primary purpose of the present investigation was to examine the true significance of the nonunique solution predicted for the truss in Fig. 1. We considered first the effect of a small misalignment of load as evidenced by a horizontal component αP. The solution now was not only unique for all nonzero α, but approached a unique limit as α tended to zero through either all-positive or all-negative values. However, these limits were different, so that in effect the nonunique solution at $\alpha = 0$ has simply been replaced by a discontinuity at $\alpha = 0$. Further, it seems evident that similar results would have been obtained had we varied various other physical parameters such as yield stress or Young's modulus or geometrical quantities such as node position or cross-sectional area.

The inclusion of nonlinear geometric terms in the equilibrium equations represents a quite different philosophical approach. Whereas previously we had *added* a small perturbation to the model, in effect allowing for experimental error, we now *restored* a nonlinear effect which normally exerts an entirely negligible effect on the solution. The results were to make all transitions smooth and unique. As α tended to zero from either direction the horizontal displacement also tended to zero, and a direct solution with $\alpha=0$ encountered no singularity but gave the unique solution $u=0$. Thus our implicit faith in the uniqueness and continuity of nature is confirmed, and the apparent singular behavior described in Sections 3 and 4 is merely the result of an oversimplified model of reality.

However, the answer above is really a mathematician's answer, and perhaps gives a misleading picture of reality to the engineer. Figure 4 was drawn with nonlinear scales to emphasize the difference between the discontinuous nonunique features of the MNO model and the unique continuous ULF model. Figure 7 shows the same information on a linear scale. Although the dashed curve for the ULF model is actually continuous through $\alpha=0$, a variation of α from -0.005 to $+0.005$ essentially changes u from -2.0 to $+2.0$, whereas except near $\alpha=0$ a change of 0.01 in α only produces a change of 0.3 in u. Thus, two experiments designed to have $\alpha=0$ might well produce experimental values of $+2$ and -2 in u due to an error of half of one percent.

From another viewpoint, $\alpha=10^{-3}$ represents deviation of less than 0.06 from the vertical in the load direction. According to Fig. 3, at stage $2L$ when the yield-point load is reached, $u=1$ and $v=3$ so that the total deviation of the loaded point from the vertical is more than 18 deg or some 300 times that of the load deviation.

In conclusion, for this simple example and considering variations in only one of the many parameters, we have shown that the linear equilibrium equations in the undeformed position produce a discontinuity and nonuniqueness which is mathematically disturbing but which is a very good approximation to physical reality. The nonlinear equilibrium equations in the deformed position produce a mathematically unique continuous solution, but one which exhibits such large changes over such a small range that the solution would be regarded as discontinuous from a practical engineering view point.

One must always be cautious about generalizing from a particular example. However, it is usually true that any phenomenon which is found in a simple example should be regarded as a possibility in a more general situation, whereas a particular technique which works in a particular case may or may not apply more generally.

If uniqueness of solution is important, it should not be assumed without evidence beyond the elastic limit. In particular, if an all-purpose computer program gives a message of termination, the possibility that the yield-point load is not yet reached should at least be considered. An empirical method of approach would be to introduce various small parameters of arbitrary sign and observe if any of them produce large effects on the solution.

The use of a numerical method which accounts for nonlinear geometric effects will almost certainly give better behaved results, but even here it would be wise to ask questions about the possibility of small changes in the problem making large differences in the results. Finally, one should always interpret the physical significance of any predicted anomalous effects. If a small change in input data truly produces a large change in an important output result, then the proposed structure is probably not a satisfactory one.

References

ADINA, 1981, "A Finite Element Program for Automatic Dynamic Incremental Nonlinear Analysis," ADINA Engineering Report AE 82-1, Watertown, Mass.

Bathe, K. J., 1982, *Finite Element Procedures in Engineering Analysis*, Prentice-Hall, Englewood Cliffs, N.J.

Freudenthal, A. M., 1954, "Effect of Rheological Behavior on Thermal Stresses," *Journal of Applied Physics*, Vol. 25, pp. 1110–1117.

Hodge, P. G., Jr., 1958, "The Practical Significance of Limit Analysis," *Journal of the Aero/Space Sciences*, Vol. 25, pp. 724–725.

Hodge, P. G., Jr. and White, D. L., 1980, "Examples of Nonuniqueness in Contained Plastic Deformation," ASME Journal of Applied Mechanics, Vol. 47, pp. 273–277.

Prager, W., 1948, "Problem Types in the Theory of Perfectly Plastic Materials," *Journal of the Aeronautical Sciences*, Vol. 15, pp. 337–341.